Thermochimica Acta, 156 (1989) 299–312
Elsevier Science Publishers B.V., Amsterdam – Printed in The Netherlands

SOLID–LIQUID EQUILIBRIA IN *PARA-/META*-XYLENE AND *PARA-/ORTHO*-XYLENE BINARY MIXTURES AT ATMOSPHERIC PRESSURE

R. DE GOEDE * and G.M. VAN ROSMALEN

Delft University of Technology, Laboratory for Process Equipment, Leeghwaterstraat 44, 2628 CA Delft (The Netherlands)

G. HAKVOORT

Delft University of Technology, Laboratory of Physical Chemistry, Julianalaan 136, 2628 BL Delft (The Netherlands)

(Received 1 May 1989)

ABSTRACT

Solid–liquid equilibria in binary mixtures of either *ortho*- and *para*-xylene or *meta*- and *para*-xylene were determined by means of differential scanning calorimetry (DSC). In both cases, the mixtures could be adequately described assuming ideal behaviour in the liquid phase and the formation of an eutectic with pure solid *para*-xylene. At high cooling rates, however, metastable miscibility in the solid phase turned out to be possible.

INTRODUCTION

In industrial practice, *p*-xylene serves mainly as an intermediate for the production of poly(ethylene terephthalate) [1]. In this process *p*-xylene is first converted into terephthalic acid or dimethyl terephthalate by oxidation, and a reaction with ethylene glycol follows. Poly(ethylene terephthalate) is used for the production of fibres, films and resins.

The major source of *p*-xylene is crude oil. In the refinery process, the aromatics are separated from the non-aromatics by sulfolane extraction, and further separation is carried out by distillation. Isomeric mixtures, however, cannot be separated adequately by distillation because their boiling points are too close. A typical C_8 aromatic mixture consists of 50% *m*-, 11% *o*- and 23% *p*-xylene and 15% ethylbenzene, with a small amount of toluene

* Author to whom correspondence should be addressed. Present address: Mannesmann Anlagenbau AG, Messo Chemietechnik, Theodorstraße 90, D-4000 Düsseldorf 30, F.R.G.

0040-6031/89/$03.50

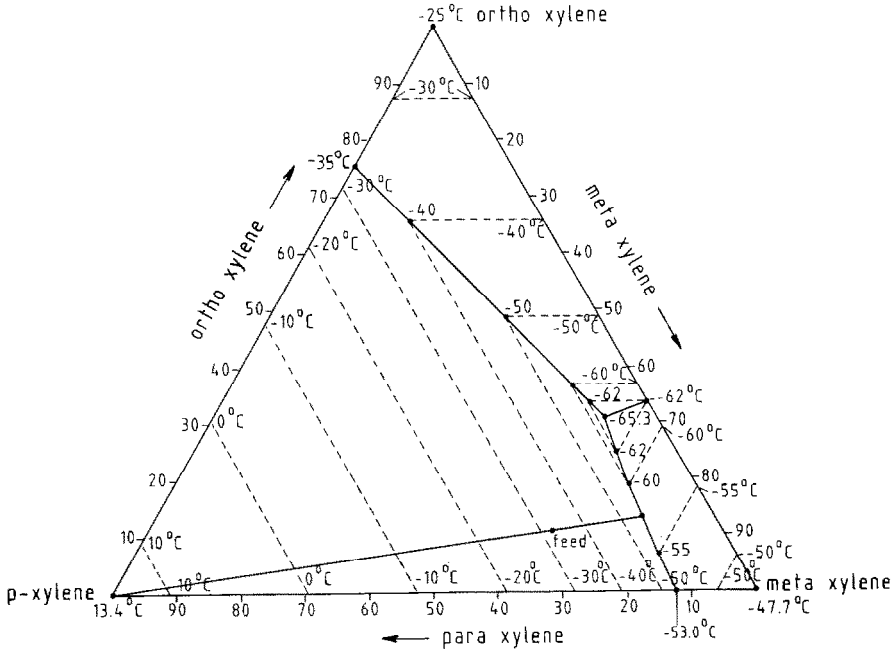

Fig. 1. Temperature projection diagram of the ternary xylene mixture assuming ideal behaviour of the liquid phase and pure solid phases.

($\approx 1\%$). Although the modern trend is to separate these products by molecular sieve adsorption, crystallization is still the most widely applied method owing to its simplicity and low energy input.

Various processes for crystallization of *p*-xylene have been developed [2–5]. Upon cooling, *p*-xylene is the first component to crystallize, and the process is limited by the temperature at which *m*-xylene starts to crystallize as well. The crystallization of *p*-xylene is usually carried out in two or more stages, followed by solid–liquid separation by centrifuge. For development and design purposes, it is generally assumed that the C_8 aromatics behave like an ideal mixture, and that the solid phases consist only of pure components. The limitations of the process are shown in a calculated ternary (*o*-, *m*- and *p*-xylene) temperature projection diagram. As far as the crystallization of *p*-xylene is concerned, non-xylene compounds (ethylbenzene and toluene) are considered to behave similarly to *o*- and *m*-xylene [2]. Ideality of the liquid phase is consistent with this assumption, because in an ideal mixture the crystallization temperature is a function of the concentration only and does not depend on the nature of the other components present. A phase diagram based on the assumptions mentioned above is presented in Fig. 1. The melting points of the pure components are given at the corners. Eutectic data of the binary mixtures are presented on the edges. From these eutectic points, three-phase lines (liquid and two solid phases) of the ternary system connect points of lower temperatures at increasing

concentrations of the third components. These three-phase lines intersect at the ternary eutectic point, which is invariant. The dashed lines are isotherms, which represent the boundaries of two-phase solid–liquid regions. On these isotherms lie a series of liquid compositions, which, at the temperature of the isotherm, are in equilibrium with the solid compound at the corner. The solid line through the *p*-xylene corner and the point indicated as 'feed' represents the mass balance of *p*-xylene during the crystallization process. While crystallizing *p*-xylene, the composition of the liquid phase shifts along this line, from the feed point to the *m*-xylene-/*p*-xylene eutectic line.

OBJECTIVE OF THE INVESTIGATION

Haddon and Johnson [6] and Porter and Johnson [7] have reported solubility data of *p*-xylene in C_8 aromatic mixtures. Significant deviations from ideal behaviour were observed in the temperature range of technical importance (-40 to $-65\,^{\circ}C$). The only explanation for these deviations is that the assumptions of an ideal liquid phase and pure solid phases are not correct. Experimental data of heats of mixing in the liquid phase have been reported in the literature [8–10]; the magnitude of these effects is, however, too small to be significant. Hence the assumption of pure solid *p*-xylene might not be valid. So far, no experimental proof of the purity of the solid phases has been reported in the literature. Moreover, unpublished results from measurements of solid–liquid equilibria of *p*-/*m*-xylene and *p*-/*o*-xylene binary mixtures performed elsewhere indicate strong miscibility in the solid phases. Because the formation of solid solutions would have a negative influence on the purity of the product and hence requires additional purification of the *p*-xylene produced by crystallization, this study was initiated to reveal whether miscibility in the solid phases may occur and, if so, to what extent.

SET-UP OF THE INVESTIGATION

The experimental determination of solid–liquid equilibria by analyzing the phases in equilibrium with each other is a time-consuming and somewhat unreliable method. First, the time needed for equilibration is unknown, but is at least a couple of hours. Second, analysis of the phases requires solid–liquid separation, and the presence of liquid attached to the solid phase can hardly be avoided. For this reason we used DSC (differential scanning calorimetry) [11], because this technique is relatively fast and no analysis of the phases is required. The principles of this technique are described in the following paragraph. Because DSC curves of multicomponent systems are difficult to interpret, binary mixtures of *o*- and *p*-xylene

and *m*- and *p*-xylene were chosen as indicative systems. Measurements on binary mixtures of *p*-xylene with ethylbenzene and toluene were not possible because such measurements require cooling to −150 °C, which is not feasible with the DSC equipment described here.

DESCRIPTION OF SOLID–LIQUID EQUILIBRIA OF BINARY XYLENE MIXTURES

To obtain crystallization process design data, phase diagrams are used in which the solubilities were calculated from the following equation [2]:

$$\ln x_i = \frac{\Delta H_{m,i}}{R}\left(\frac{1}{T_{m,i}} - \frac{1}{T}\right) + \frac{\Delta C_{p,i}}{R}\left(\ln \frac{T}{T_{m,i}} + \frac{T_m}{T} - 1\right) \quad (1)$$

where x_i is the mole fraction of component i in the liquid phase; $\Delta H_{m,i}$ is the latent heat of melting of component i; $T_{m,i}$ is the melting temperature of the pure component i; T is the equilibrium melting temperature at mole fraction x; $\Delta C_{p,i}$ is the difference in heat capacities of pure, hypothetical subcooled liquid and pure solid component i, $C_{p,L,i} - C_{p,S,i}$, both at temperature T; R is the gas constant, 8.3144 J mol^{-1} K^{-1}. In the derivation of eqn. (1), the following assumptions are made.

(i) The difference in heat capacities of the pure component i in the liquid and the solid phase, ΔC_p, is independent of temperature.

(ii) The liquid phase behaves like an ideal mixture

(iii) The solid phases are pure.

A binary T,x cross-section of a system that obeys the foregoing assumptions can be constructed using eqn. (1) for both components. The eutectic temperature and composition follow from a simultaneous solution of eqn. (1) for both components. Schematically, such a T,x cross-section is shown in Fig. 2. For the binary xylene mixtures described in this paper, such T,x cross-sections can also be predicted from eqn. (1). The calorific data of the pure components as well as the eutectic coordinates calculated from eqn. (1) are summarized in Table 1.

Krawtschenko [15] has previously compared calculated eutectic data with experimental values from the literature. His findings were as follows. The data of Kijner and Wendelstein [16] were in good agreement with the calculated eutectics. Data published by Nakatsuchi [17,18] also agreed well in the case of *o*-/*p*-xylene, but showed significant deviations in the case of *m*-/*p*-xylene. This is probably because the *m*-xylene he used was relatively impure.

A schematic representation of the expected DSC heating curves for this type of phase behaviour is given in Fig. 3. It is assumed that the initial temperature is low enough to start with a completely solid sample, and that the sample weight is equal for all three DSC curves. Curve I results from a

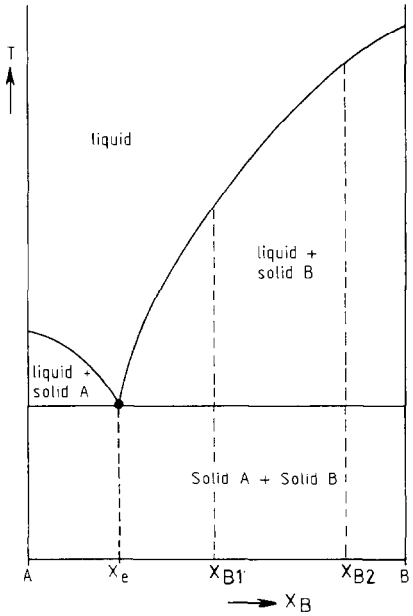

Fig. 2. Schematic T,x cross-section for an ideal mixture with pure solid phases. The eutectic composition is denoted by x_e.

sample with an overall composition equal to the eutectic composition. In this case the entire sample will be converted into liquid at the eutectic temperature, so only one peak will be observed. The second curve results from a mixture with an overall composition containing more *p*-xylene than the eutectic one. Here, the peak at the eutectic temperature will be smaller because the part of the *p*-xylene present melts in the temperature range between the eutectic temperature and the liquidus. At the temperature of the liquidus, all the *p*-xylene is molten and the peak returns to the baseline. A mixture richer in *p*-xylene yields the third curve: the eutectic peak will be smaller again and the second peak ends at a higher temperature.

TABLE 1

Thermodynamic properties of *o*-, *m*- and *p*-xylene and calculated eutectics of *o*-/*p*-xylene and *m*-/*p*-xylene binaries. T_e is the eutectic temperature, and x_e is the mole fraction of *p*-xylene in the eutectic mixture. References are given in square brackets

Component	T_m (K) [12]	ΔH_m (J mol^{-1}) [13]	ΔC_p (J mol^{-1} K) [14]	T_e (K)	x_e
o-Xylene	247.968	13598	27.6	} 237.824	0.243
p-Xylene	286.413	17113	24.3		
m-Xylene	225.278	11569	40.2	} 220.303	0.129

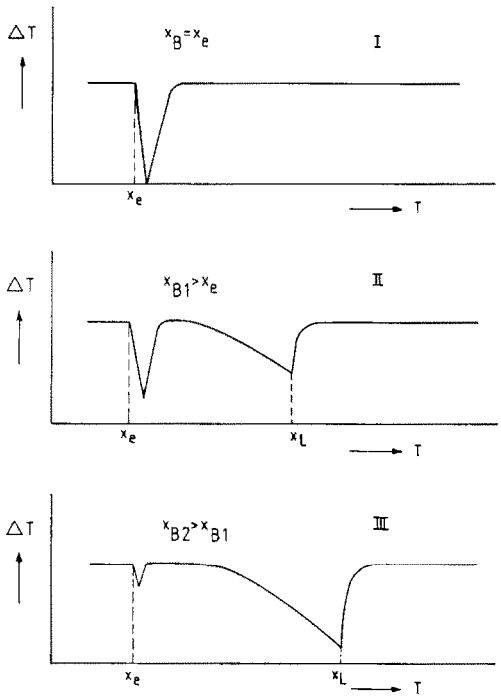

Fig. 3. Schematic representation of the expected DSC curves resulting from a binary mixture with phase behaviour as shown in Fig. 2.

So far, only the simplest type of phase behaviour has been discussed. Many other types of phase diagram are, however, encountered in systems where solid solutions are formed [19]. It will be obvious that DSC curves for these types of system will differ from those presented in Fig. 3. Conversely, experimentally determined DSC curves may serve to construct the phase diagram of a certain system. Because of the applied cooling rate, this does not necessarily lead to the equilibrium phase diagram, as will be seen from the results presented in this paper.

EXPERIMENTAL

Chemicals

The *o*-, *m*- and *p*-xylene were all purchased from J.T. Baker, as chemically pure-grade compounds of purity $\geqslant 99\%$ weight. Analysis by gas chromatography using a bentonite column demonstrated that the *o*- and *m*-xylene contained no detectable amounts of *m*-purities. The *p*-xylene contained about 1% of *m*-xylene.

Equipment

The apparatus used is a Du Pont 910 differential scanning calorimeter system [20]. For experiments at low temperatures, a special bell jar was applied, fitted with a Dewar vessel that could be filled with liquid nitrogen. The samples were encapsulated in hermetically sealed pans.

Procedure

First, the weight of the cup was determined. After inserting a sample of the desired composition (20–30 mg) the cup was closed and sealed. The weight of sample and cup together was determined and the sample weight was calculated by subtraction. Subsequently, the sample was inserted in the apparatus, then the cooling vessel was installed and filled with liquid nitrogen. Cooling was possible either uncontrolled or with programmed rates. In all cases, the sample was cooled to $-100\,^{\circ}C$ while measuring the DSC curve. Heating was always effected at a rate of $2\,^{\circ}C\ min^{-1}$ with measurement of the DSC curve. During all experiments the cell was purged with nitrogen.

At first, cooling was performed at an uncontrolled rate, which was approximately $4\,^{\circ}C\ min^{-1}$. Because of the poor reproducibility of these measurements, it was decided to cool the sample at lower, programmed rates. DSC curves were recorded only for mixtures in the *p*-xylene-rich region ($0.7 < x < 1$) because of their relevance for our purposes.

RESULTS AND DISCUSSION

Types of thermograms

The thermograms resulting from heating of the samples can be divided into three types, which are schematically presented in Fig. 4. Type I usually results from experiments performed at low cooling rates. The onset temperature of the first peak corresponds with the expected value of the eutectic temperature. Type III is usually obtained when high cooling rates are applied, and the first peak appears at much lower temperatures. Type II occurs only occasionally and mainly at low cooling rates.

The explanation for the occurrence of these three types of heating curves is that, depending on the cooling rate, a stable as well as a metastable solid phase can be formed. Upon cooling at a low rate, the stable state is usually formed. Heating then results in a DSC curve of type I. Even if a metastable state is formed in spite of the low cooling rate, enough nuclei of the stable state are available to induce the transformation from the metastable into the stable state upon heating. This leads to a DSC curve of type II. The

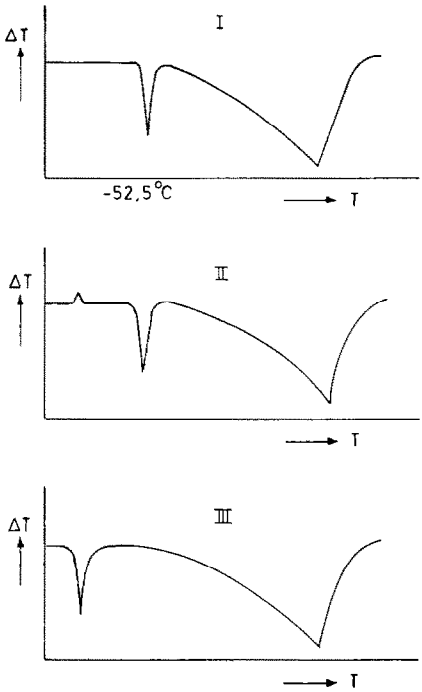

Fig. 4. Schematic representation of the three different types of thermograms resulting from the experiments with mixtures of *p*-xylene and *m*-xylene. Type I, cooled to a stable state; type II, cooled to a metastable state with transition into a stable state; type III, cooled to a metastable state without transition into a stable state.

exothermic peak observed in such curves results from the transition of the metastable into the stable state. This statement is supported by the fact that, after the occurrence of an exothermic peak, the first endothermic peak always corresponds with the expected value of the eutectic temperature. High cooling rates usually result in a metastable state. Under such conditions no nuclei of the stable state are formed because of low diffusivities in comparison with the cooling rate and short exposure time in the temperature region of interest. Melting now occurs at temperatures below the eutectic value, which results in a type III DSC curve.

The m-/p-xylene system

From all DSC heating curves of the *m*-/*p*-xylene system, the onset temperatures of the first endothermic peaks were determined and the peak temperatures of the second ones. Temperatures derived from type I and type II DSC curves are represented by open circles and those from type III DSC curves are represented by crosses. The results are shown in Fig. 5. The continuous lines in Fig. 5 are calculated from eqn. (1). The measurements

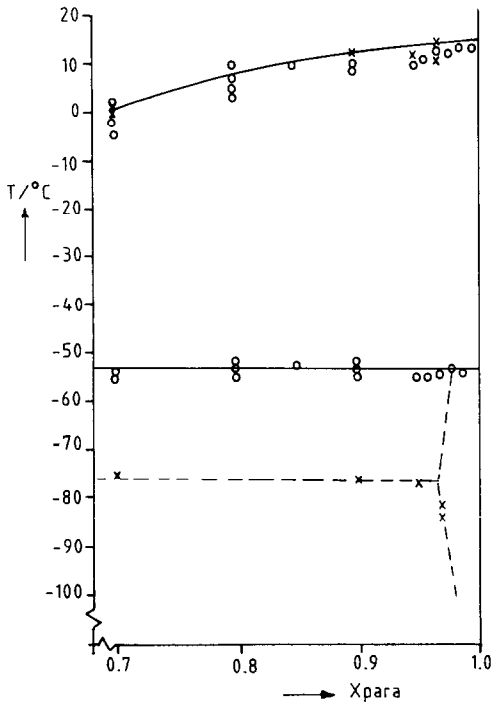

Fig. 5. The onset temperatures of the first peaks and the peak temperatures of the second peaks from DSC curves of *m*-/*p*-xylene. o, temperatures from type I and II DSC curves; ×, temperatures from type III DSC curves.

from DSC curves of type I and II appear to be in good agreement with the calculated lines, and thus with the assumptions of both ideality of the liquid phase and a solid phase consisting of pure *p*-xylene. The scatter here is probably larger than in the data reported by Haddon, Porter and Johnson [6,7], but it should be stressed here that our measurements serve only to construct the shape of the phase diagram and are not meant for accurate determination of solubilities. The scatter of DSC data can probably be ascribed to changes in the composition of the sample upon partial evaporation. The measurements from the type III DSC curves suggest miscibility in the solid phase. The most likely shape of the metastable phase diagram as derived from these data is given in the figure by dashed lines.

So far, we have been dealing only with the concentration region between 70 and 100% *p*-xylene. The expected shape of the complete phase diagram is presented in Fig. 6, where the speculative phase boundaries are given by discontinuous lines.

The stable equilibria are expected to obey the assumptions of ideality in the liquid phase and pure solid phases, but for the metastable system a limited miscibility in the solid phases is expected, although miscibility in the

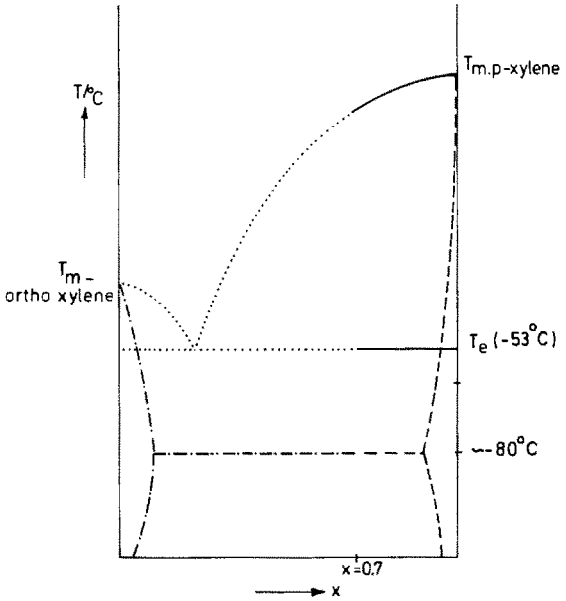

Fig. 6. Phase diagram of *m-/p*-xylene. ———, Stable states, x between 0.7 and 1; — — —, metastable states, x between 0.7 and 1; ····· stable states, x between 0 and 0.7; ·–·–·, metastable states, x between 0 and 0.7.

solid phase has been supported by experimental evidence only in the concentration region $0.7 < x < 1$.

The o-/p-xylene system

The results of measurements on the *o-/p*-xylene system are presented in Fig. 7. Because the stable and metastable states are not as clearly distinguishable as for the *m-/p*-xylene system, all measured temperatures are given here by open circles. The continuous lines, as calculated from eqn. (1), again represent ideal behaviour in the liquid phase and a eutectic with pure *p*-xylene. The measured values of the peak temperatures of the second peak agree well with the calculated liquidus, but most of the points at lower temperatures, as obtained from the same heating curves, do not correspond with the eutectic temperature. This apparent inconsistency can be assigned to the fact that the *p*-xylene we used was contaminated with a low percentage of *m*-xylene. This implies that we are actually dealing with the ternary xylene mixture. The effect of the impurity upon the position of the eutectic line is illustrated in Fig. 8, where the ternary mixture is treated as a pseudo-binary mixture with *o*-xylene being the first component and the *m-/p*-xylene mixture of fixed composition as the second.

The heavily dashed line in the ternary diagram represents all the overall compositions of mixtures of *o*-xylene and the *para–meta* mixture. The

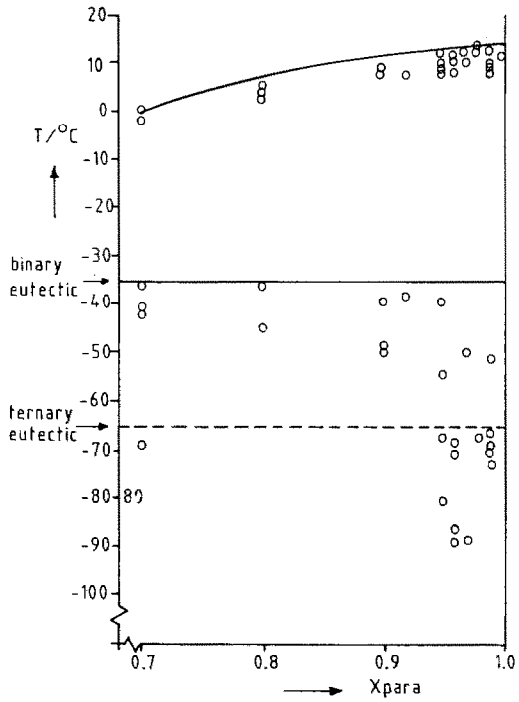

Fig. 7. The onset temperatures of the first peaks and the peak temperatures of the second peaks from DSC curves of *o*-/*p*-xylene.

lightly dashed lines represent mass balances and the composition of the liquid phase in equilibrium with solid *p*-xylene shifts along this line. It is obvious that the eutectic temperature decreases with decreasing *o*-xylene concentration, and that this effect becomes more significant with decreasing *o*-xylene concentration because the relative amount of *m*-xylene increases. In principle, the onset of a peak should always be observed at the ternary eutectic temperature due to the melting of *m*-xylene. Since, however, the amount of *m*-xylene impurity is only 10% of the *o*-xylene concentration at a *p*-xylene concentration of 90 °C, it is not surprising that the onset of the melting curve at the eutectic temperature was only observable in the concentration range between 90 and 100%. These peaks are not sharp because, after the melting of *m*-xylene, the *o*-xylene immediately starts to melt. In the range where the *m*- and *o*-xylene concentrations are of the same order of magnitude (98–99%), a double peak was visible.

So far, the tendency towards lower temperatures with increasing *p*-xylene concentrations has been explained. The occurrence of peaks at considerably lower temperatures than the ternary eutectic can be explained by the existence of a metastable solid phase. From these measurements it is not feasible to predict the shape of a diagram which includes the metastable

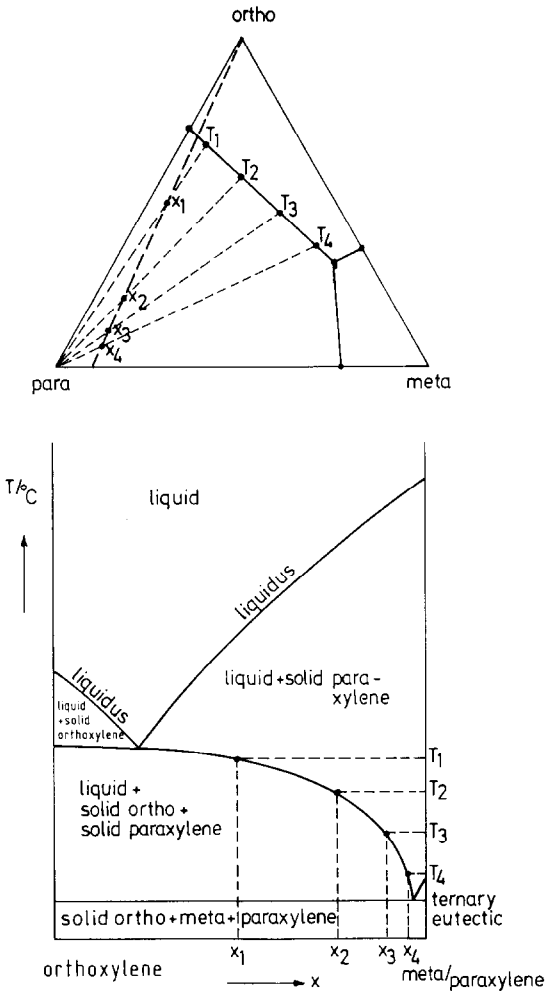

Fig. 8. The construction of a pseudo-binary cross-section from the ternary diagram.

equilibria. The stable equilibria are again expected to obey the conditions of ideality of the liquid phase and purity of the solid phases.

CONCLUSIONS

The results described above can be summarized in the following observations.

(i) At high cooling rates (4 °C min^{-1}) a metastable solid state is frequently formed upon complete freezing of the sample.

(ii) In the case of *m*-/*p*-xylene mixtures, total freezing at lower cooling rates (0.5 °C min^{-1}) usually gives a stable solid state. Even if a metastable

solid phase is formed, sufficient nuclei are present to induce the transformation of the metastable into the stable state. This tendency is less obvious for *o-/p*-xylene mixtures.

(iii) No stable solid solutions have been identified. Metastable miscibility in the solid state appears, however, to be possible.

(iv) Within the accuracy of our experiments, equilibria between the liquid and the stable solid phase are consistent with the usual assumption of ideality in the liquid and pure solid phases. In the *m-/p*-xylene system, experimental data agree well with the predicted phase diagram. In the *ortho–para* system, the deviations can be explained by the presence of some *m*-xylene as an impurity in *p*-xylene.

(v) As a conclusion we find that, in industrial processes, instantaneous cooling should be avoided because formation of metastable solid solutions decreases the purity of the product.

ACKNOWLEDGEMENTS

The authors thank Esso Chemie Nederland b.v. for their financial support. They are also grateful to Mr. J. te Nijenhuis and Mrs. J. Dvořáková for their contributions to the experimental work. They thank Professor E.J. de Jong for the stimulating discussion.

LIST OF SYMBOLS

C heat capacity at constant pressure (J mol^{-1} K^{-1})
H enthalpy (J mol^{-1})
R gas constant (J mol^{-1} K^{-1})
T temperature (K, °C)
t time (s)
x mole fraction

Greek symbols

Δ differential signal

Subscripts

e eutectic
i arbitrary component
m melting
L liquid
S solid

REFERENCES

1 Kirk-Othmer Encyclopedia of Chemical Technology, Wiley, New York, 3rd edn., 1984.
2 D.L. McKay, G.H. Dale and D.C. Tabler, Chem. Eng. Prog., 62 (1966) 104.
3 A.G. Duncan and R.H. Phillips, Trans. Inst. Chem. Eng., 54 (1976) 153.
4 T. Amemiya, Y. Hatanaka and T. Nakamura, Bull. Jpn. Pet. Inst., 16(1) (1974) 43.
5 J.E. Clark and R.V. Luthy, Ind. Eng. Chem., 47 (1955) 250.
6 W.F. Haddon and J.F. Johnson, J. Chem. Eng. Data 9(1) (1964) 158.
7 R.S. Porter and J.F. Johnson, J. Chem. Eng. Data 12(3) (1967) 392.
8 J.L. Fortier and G.C. Benson, J. Chem. Eng. Data 25(1) (1980) 47.
9 D.L. Holt and B.D. Smith, J. Chem. Eng. Data 19(2) (1974) 129.
10 V.T. Lam, S. Mirakami and G.C. Benson, J. Chem. Thermodyn., 2 (1970) 17.
11 W. Wendlandt, W., Thermal Methods of Analysis, Wiley, New York, 2nd Edn., 1974.
12 N.B. Vargaftik, Tables on the Thermodynamical Properties of Liquids and Gases, Wiley, New York, 2nd Edn., 1975.
13 R.H. Perry and C.H. Chilton, Chemical Engineers Handbook, McGraw-Hill, Kogakusha, 5th Edn., 1973.
14 K.S. Pitzer and D.W. Scott, J. Am. Chem. Soc., 65 (1943) 803.
15 W.M. Krawtschenko, Acta Physicochim. U.S.S.R., 14(2) (1941) 279.
16 N. Kijner and G. Wendelstein, J. Russ. Chem. Phys. Soc., 57(1) (1925).
17 A. Nakatsuchi, J. Chem. Ind. Jpn., 29 (1926) 29.
18 A. Nakatsuchi, J. Chem. Ind. Jpn., 32 (1929) 1081.
19 F. Rosenberger, Fundamentals of Crystal Growth, Springer-Verlag, Berlin, 1979.
20 Instruction Manual for DSC system 910, Du Pont Co.